

High and low frequency Alfvén modes in tokamaks

S. Briguglio, L. Chen^a, Jiaqi Dong^b, G. Fogaccia, R.A. Santoro^c,
G. Vlad, F. Zonca

Associazione Euratom–ENEA sulla Fusione,
Frascati, Rome, Italy

^a Department of Physics and Astronomy, University of California,
Irvine, California, United States of America

^b Southwestern Institute of Physics,
Chengdu, China

^c Naval Research Laboratory,
Washington, D.C., United States of America

Abstract. The article presents an analysis of the typical features of shear Alfvén waves in tokamak plasmas in a frequency domain ranging from the ‘high’ frequencies ($\omega \cong v_A/2qR_0$, where v_A is the Alfvén speed and qR_0 is the tokamak connection length) of the toroidal gap to the ‘low’ frequencies, comparable with the thermal ion diamagnetic frequency ω_{*pi} and/or the thermal ion transit frequency $\omega_{ti} = v_{ti}/qR_0$ (where v_{ti} is the ion thermal speed).

1. Ideal MHD TAE spectrum in ITER

In recent years, the shear Alfvén wave spectrum in laboratory plasmas has been extensively analysed because of the possible excitation of these waves by resonant interactions with energetic particles such as charged fusion products and ions accelerated by plasma heating or current drive systems. In particular, great attention has been devoted to the plasma eigenmodes near the frequency gap [1] in the shear Alfvén continuous spectrum, i.e. toroidal Alfvén eigenmodes (TAEs) [2] and kinetic toroidal Alfvén eigenmodes (KTAEs) [3], respectively.

Although a numerical approach to TAE and KTAE linear stability in a realistic plasma equilibrium is necessary, there still remain some concerns about the actual solution of this problem. In fact, in a tokamak reactor of major radius R_0 and minor radius a , the most unstable Alfvén modes will be characterized by toroidal mode numbers n in the range $a/\rho_{LE} \gtrsim n \gtrsim \epsilon a/\rho_{LE} \gg 1$, where $\epsilon = a/R_0$ and ρ_{LE} is the energetic particle Larmor radius. The large mode numbers create serious resolution problems for conventional numerical simulations of these instabilities; however, significant insights can still be obtained with studies based on analytical–theoretical methods. Previous analyses — using a 2-D WKB code [4] — have studied this problem

either for (s, α) [5] (s being the magnetic shear and $\alpha = -q^2 R_0 \beta'$) model equilibria or for more general (but still model) equilibria, including possible shaping of magnetic flux surfaces [6]. In the former case, the fairly simple model equilibrium allowed us to focus on the details of the energetic particle dynamics and thus on the destabilization mechanism due to wave–particle interactions, whereas in the latter case, a more precise description of the wave spectra in realistic geometries was obtained at the price of neglecting the energetic particle drive and all wave–particle resonant interactions, i.e. the result consists of calculations of a marginally stable set of global eigenmodes.

These investigations have confirmed that, under certain plasma conditions, TAEs can be shifted downward in frequency and out of the toroidal frequency gap in the Alfvén continuum. As a consequence, there is a great increase in the mode damping due to finite coupling to the continuous spectrum. For high n and the (s, α) model equilibrium [5], this has been shown to occur for $\alpha > \alpha_c(s)$ [7–9], i.e. above a critical threshold in the thermal plasma pressure gradient. In the present work, we further extend the approach of Ref. [6] and investigate the ideal MHD spectrum of high n TAEs in ITER, in order to explore the possibility of having plasma equilibria free of TAEs. The ideal MHD assumption clearly prevents us from computing the excitation

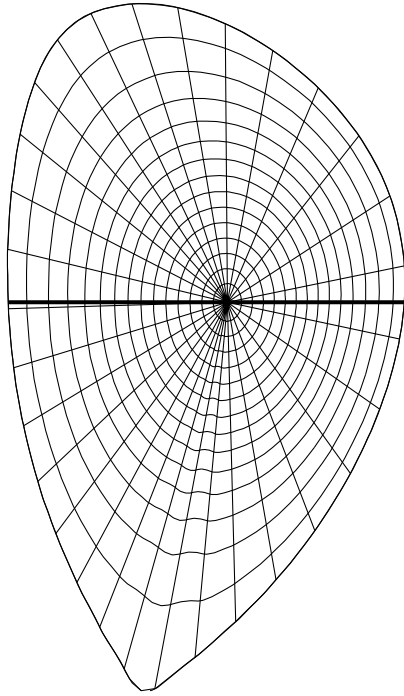


Figure 1. Constant ψ and constant poloidal angle contours for the ITER equilibrium considered, indicated as ITER reference scenario 2 for TAE stability studies.

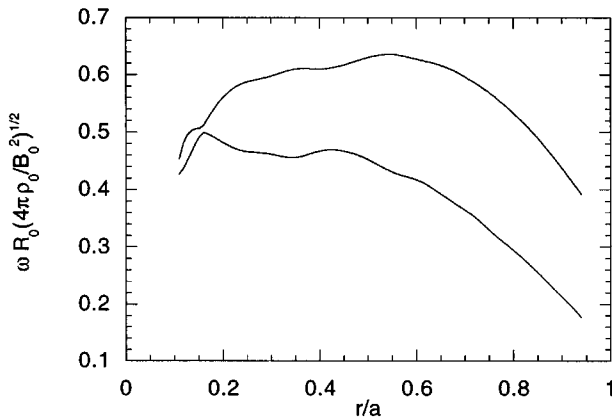


Figure 2. Radial profile of boundaries of the toroidal Alfvén gap in the continuous spectrum.

thresholds but allows us to analyse the conditions for enhanced TAE continuum damping in a realistic and completely general ITER equilibrium with shaped flux surfaces.

The plasma equilibrium we consider here is shown in Fig. 1 and is characterized by $R_0 = 8.14$ m, $a = 2.90$ m, magnetic axis position $(R, Z) = (8.44$ m, 0.66 m), elongation $\kappa = 1.73$, $B_0 = 5.68$ T, plasma current $I = 20.9$ MA, volume average beta

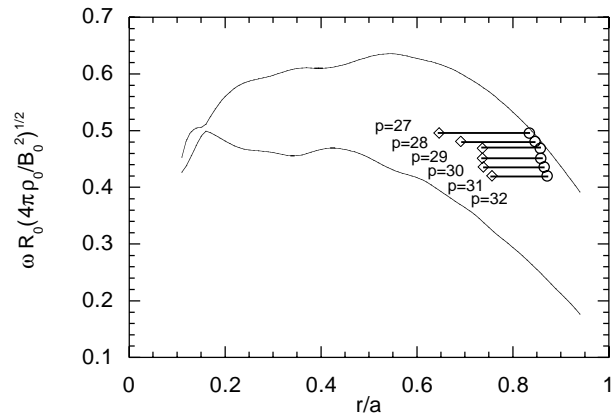


Figure 3. Ideal MHD global TAE frequency spectrum for $n = 20$. The toroidal gap boundaries are also shown.

$\langle \beta \rangle = 0.027$, poloidal beta $\beta_p = 0.69$, $q(0) = 0.84$ and $q(a) = 4.47$. Figure 2 shows the corresponding boundaries of the toroidal gap in the shear Alfvén continuous spectrum (i.e. the geometric loci of its accumulation points in the high n limit). Here and in the rest of this section, frequencies are normalized to the Alfvén frequency on-axis, $\omega_A \equiv B_0/R_0\sqrt{4\pi\rho_0}$.

The frequency spectrum of TAEs is found by solving the global dispersion relation [9]

$$\oint \theta_k(r; \omega) d(nq(r)) = (2p + w) \quad (1)$$

where $\theta_k \equiv k_r/nq'$ is the WKB eikonal entering in the expression of the radial envelope of the mode [9], p is the radial mode number and w is an integer defined in the following. The WKB eikonal θ_k is a function of the radial position, as it may be obtained from the solution of the local TAE dispersion relation

$$F(r, \theta_k; \omega) = 0 \quad (2)$$

which is parameterized by the mode frequency ω . Furthermore, the integration in Eq. (1) is extended to a complete periodic orbit (at fixed ω) in the (r, θ_k) phase space, and w is either $w = 0$ for phase space rotations or $w = 1$ for phase space oscillations. Incidentally, we note that, in the up-down asymmetric equilibrium of Fig. 1, $\theta_k = 0$ and $\theta_k = \pi$ are not WKB turning points, as in the general symmetric case, and that turning point positions need to be determined numerically from Eq. (2).

Numerical solutions of the global mode dispersion relation are shown in Fig. 3 for the toroidal mode number $n = 20$. Each global mode is represented by a horizontal segment delimited by the WKB turning point positions, which give an estimate of the

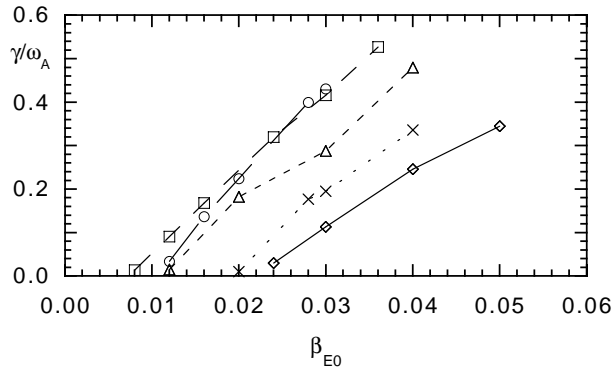


Figure 4. Normalized EPM growth rates versus β_{E0} for different toroidal mode numbers; $n = 1$ (Σ), 4 (\circ), 8 (\cdot), 12 (Δ) and 16 (\times).

corresponding radial mode width. Different eigenmodes are labelled by the radial mode number p . It is evident that the interior of the plasma discharge, (r/a) \lesssim 0.6, is free of global TAEs. As mentioned above, this fact is essentially due to finite β effects [6–9], which cause a downward TAE frequency shift and eventually a strong local interaction (continuum damping) of the mode with the shear Alfvén continuum at the radial position where the mode frequency is degenerate with that of the continuous spectrum. As to the $n = 20$ TAEs, which are shown in Fig. 3, they are expected to be both weakly driven — a low α particle energy density is expected in the outer region of the plasma discharge — and appreciably stabilized via continuum damping, because of the vicinity of their right WKB turning point to the shear Alfvén continuum. In fact, one could easily guess from Fig. 3 that the $p = 27$ radial mode number is more strongly affected by continuum damping than $p = 32$. In conclusion, TAEs are not expected to have an appreciable influence on the present ITER plasma equilibrium.

The present work also gives some indication that very localized ($0.45 \lesssim (r/a) \lesssim 0.65$) KTAEs could exist very close to the upper shear Alfvén continuum frequencies. This conclusion is a consequence of the existence of WKB turning point pairs, characterized by these frequencies and this localization, which have already merged into the continuum. The present ideal MHD theory breaks down for such modes. However, it provides an indication for the possible existence of KTAEs with such characteristics. Nonetheless, this type of very localized KTAE could have an impact on the α particle dynamics only in the narrow region in which they may be excited.

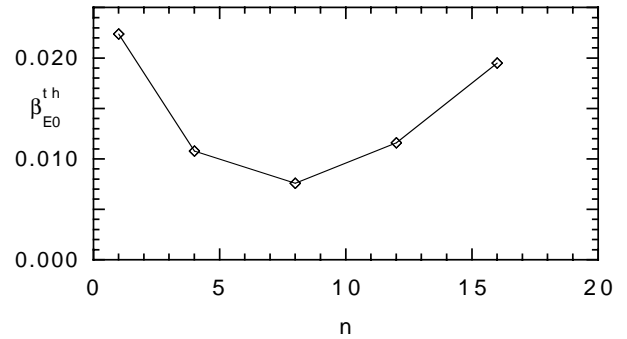


Figure 5. Dependence of EPM excitation threshold β_{E0}^{th} on toroidal mode number n .

2. Energetic particle mode dynamics

Besides the existence of eigenmodes of the thermal plasma, such as TAEs and KTAEs, it has been shown that other instabilities may be spontaneously excited by a sufficiently strong energetic particle drive [10, 11]. These energetic particle modes (EPMs) [10], due to the non-perturbative contribution of particle dynamics in determining mode structures and frequencies, have linear and non-linear behaviours which are different from those of TAEs and KTAEs. In particular, it has been demonstrated that when the particle drive is large enough to exceed the EPM threshold, a strong redistribution in the energetic particle source can take place, yielding potentially large particle losses and eventually mode saturation [6]. Previous results from numerical simulations [6, 12] indicated that the EPM excitation threshold can be fairly high at low toroidal mode numbers n , although the tendency of the threshold to decrease for increasing n was also emphasized, in accordance with theoretical expectations [13], which predicted a minimum in the excitation threshold for $n \gtrsim \epsilon a / \rho_{LE}$.

Recalling that the linear excitation threshold of EPMs also corresponds to the level above which a strong redistribution in the energetic particle source can take place, it becomes a crucial issue to investigate whether, for higher mode numbers n , the EPM excitation threshold can become comparable with the values which are relevant for an ignited plasma. In the present section, we present new results on this problem with the help of numerical simulations (moderate n ; $n \leq 16$) using a gridless finite size particle modified version [14] of the original 3-D PIC hybrid MHD–gyrokinetic code [12].

The code self-consistently evolves the coupled set of reduced MHD equations for the fluctuating electromagnetic fields, driven by an energetic particle pressure term, and the Vlasov equation for the distribution function of such particles.

Figure 4 shows the typical dependence of the EPM growth rate (normalized to ω_A) on the energetic particle β_E on-axis, β_{E0} , for different n 's. Here fixed parameters are $\epsilon = 0.1$, $q(0) = 1.1$, $q(a) = 1.9$, $\rho_{LE}/a = 0.01$ and $L_{pE}/R_0 = \epsilon(a/r)^3/16$, with $L_{pE}^{-1} \equiv |\nabla p_E|/p_E$. The existence of an excitation threshold, β_{E0}^{th} , is apparent, above which the EPM growth rate rapidly increases with β_{E0} .

The dependence of β_{E0}^{th} on the toroidal mode number n is shown in Fig. 5 and it is clearly indicated that a minimum of $\beta_{E0}^{th} \cong 7.5 \times 10^{-3}$ in the excitation threshold is reached for $n \cong 8$, for the present simulation parameters. Such a minimum threshold value should be considered as an indicative one, because it depends on the details of the specific equilibrium configuration.

3. Excitation of Alfvénic ion temperature gradient modes

When the EPM frequency — because of either thermal plasma or energetic particle compression effects [6, 11, 15] — becomes so low as to be comparable with the ion diamagnetic frequency ω_{*pi} and/or the thermal ion transit frequency $\omega_{ti} \equiv v_{ti}/qR_0$, the EPM acquires all the characteristics of the ‘beta induced Alfvén eigenmode’ (BAE) [16] and it may be considered as a good candidate to explain some experimental observations [17]. Actually, it has been demonstrated that, for $\omega_{*pi} \approx \omega_{ti}$, BAEs/EPMs cannot be considered separately from modes of the kinetic ballooning mode (KBM) [18] branch resonantly excited by energetic particles, since they are two (generally coupled) branches of the shear Alfvén wave in this frequency range [19].

The BAE/EPM and KBM/EPM dispersion relation generally reads

$$i\Lambda\left(\frac{\omega}{\omega_{ti}}\right) = \delta W_f + \delta W_E \quad (3)$$

where δW_f is the ideal MHD potential energy and δW_E is the contribution of energetic particles [19, 20]. Here $\Lambda(\omega/\omega_{ti})$ is the renormalized plasma

inertia in the presence of finite ω_{*pi} and ω_{ti} , i.e. [19]

$$\Lambda(x) = \beta_i^{1/2} \left\{ x^2 \left(1 - \frac{\omega_{*pi}}{\omega} \right) + q^2 x \left[\left(1 - \frac{\omega_{*ni}}{\omega} \right) F(x) - \frac{\omega_{*Ti}}{\omega} G(x) - \frac{N^2(x)}{D(x)} \right] \right\}^{1/2} \quad (4)$$

with

$$F(x) = x(x^2 + 3/2) + (x^4 + x^2 + 1/2)Z(x)$$

$$G(x) = x(x^4 + x^2 + 2) + (x^6 + x^4/2 + x^2 + 3/4)Z(x)$$

$$N(x) = \left(1 - \frac{\omega_{*ni}}{\omega} \right) [x + (1/2 + x^2)Z(x)]$$

$$- \frac{\omega_{*Ti}}{\omega} [x(1/2 + x^2) + (1/4 + x^4)Z(x)]$$

$$D(x) = \left(\frac{1}{x} \right) \left(1 + \frac{T_e}{T_i} \right) + \left(1 - \frac{\omega_{*ni}}{\omega} \right) Z(x)$$

$$- \frac{\omega_{*Ti}}{\omega} [x + (x^2 - 1/2)Z(x)] \quad (5)$$

where $Z(x) = \pi^{-1/2} \int_{-\infty}^{\infty} e^{-y^2}/(y-x) dy$ is the plasma dispersion function. In Eq. (3), the excitation condition for EPMS of either the BAE or the KBM branch is $\text{Re } \delta W_E \leq -\delta W_f$.

Another interesting feature of Eq. (3) is that it predicts that modes of the shear Alfvén branch may be excited even in the absence of an energetic particle drive. In fact, for $\delta W_E = 0$, it may be shown that the shear Alfvén continuous spectrum can have an unstable accumulation point ($\delta W_f = 0$) in the presence of a sufficiently strong thermal ion temperature gradient [19, 21, 22]. This fact, which stretches Eq. (3) beyond its applicability limit, is the clear indication that a discrete Alfvénic mode must exist below the marginal stability threshold for ideal MHD modes [19, 23]. In fact, the existence of a solution of $\Lambda(\omega/\omega_{ti}) = 0$ with $\text{Im } \omega > 0$ demonstrates that, at the ideal MHD marginal stability boundary ($\delta W_f = 0$), there still exists a free energy source to be tapped by instabilities, provided that ∇T_i is sufficiently strong.

Since, at $\delta W_f = 0$, the mode structure tends to become highly localized in the radial direction (singular within ideal MHD), finite ion Larmor radius (FLR) and finite drift orbit width (FOW) effects become crucial to demonstrate that unstable discrete modes can actually exist for $\delta W_f > 0$. In fact, it is possible to show that these instabilities may be interpreted as a discretization of the unstable continuum due to FLR and FOW effects [23]. Since they

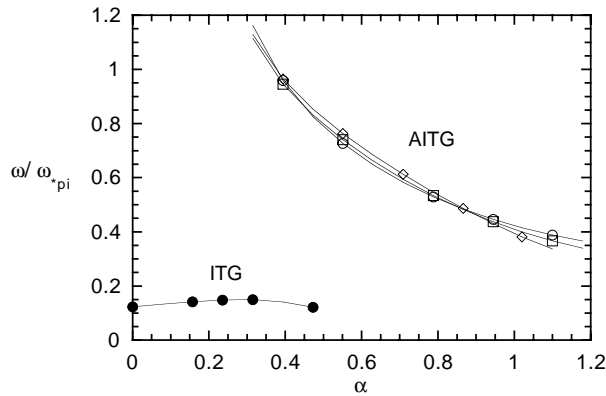


Figure 6. Real mode frequencies of the AITG are shown versus α for three different values of $\eta_i = 0.5$ (\circ), 1.0 (\square) and 2.5 (Σ). Fixed parameters are $s = 1$, $q = 1.5$, $k_\theta \rho_{Li} = 0.3$, $T_e/T_i = 1$, $\eta_e/\eta_i = 1$ and $L_{pi}/R_0 = 0.057$. The electrostatic ion temperature gradient mode (\bullet) is also shown for $\eta_i = 2.5$.

are characterized by a shear Alfvén polarization and require ∇T_i to exceed a threshold value, they may be called shear Alfvén ∇T_i eigenmodes (AITGs) [23], in analogy to their electrostatic counterpart. Using the (s, α) [5] model equilibrium for tokamak plasmas with shifted circular magnetic flux surfaces, we studied the problem of AITG excitation for $\delta W_f > 0$, using a set of integral eigenmode equations (quasi-neutrality and vorticity), which allow us to handle arbitrary $k_\perp \rho_i$ (FLR) and $k_\perp \rho_d$ (FOW).

Numerical solutions of the coupled integral equations for the two fields ($\delta\phi, \delta A_\parallel$) indicate that the growth rate of AITGs is maximum for $k_\theta \rho_{Li} \approx 0.3$, where k_θ is the poloidal wave vector and ρ_{Li} is the thermal ion Larmor radius. Figures 6 and 7 show, respectively, the real and imaginary parts of the AITG frequency, normalized to ω_{*pi} , versus α for three different values of $\eta_i = 0.5, 1.0$ and 2.5 . Fixed parameters are $s = 1$, $q = 1.5$, $k_\theta \rho_{Li} = 0.3$, $T_e/T_i = 1$, $\eta_e/\eta_i = 1$ and $L_{pi}/R_0 = 0.057$, with $L_{pi}^{-1} \equiv |\nabla p_i|/p_i$. For reference, the ‘electrostatic’ ion temperature gradient mode (ITG) is also shown for $\eta_i = 2.5$.

It is apparent that the AITG instability can exist well below $\alpha_{crit} \cong 0.62$, the stability threshold for ideal ballooning modes [5], and that it is actually stronger than the usual electrostatic ITG for $0.4 - 0.5 \lesssim \alpha/\alpha_{crit} \lesssim 1$. This fact can be explained by considering the stabilizing influence of magnetic field line bending. In fact, approaching MHD marginal stability, line bending stabilization is nearly balanced by the ballooning destabilization and the

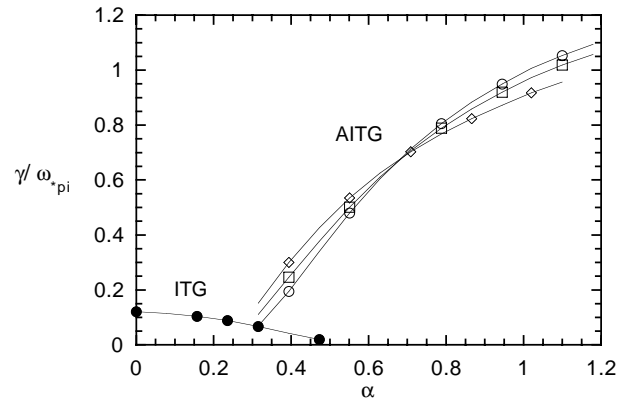


Figure 7. Imaginary mode growth rates of the AITG are shown versus α for three different values of $\eta_i = 0.5$ (\circ), 1.0 (\square) and 2.5 (Σ) for the same parameters as in Fig. 6. The electrostatic ion temperature gradient mode (\bullet) is also shown for $\eta_i = 2.5$.

AITG is unstable because of the free energy available at the unstable continuum accumulation point. For $\alpha < \alpha_{crit}$, i.e. $\delta W_f > 0$, line bending stabilization becomes increasingly effective, and the AITG is eventually completely stabilized.

Line bending, as is well known, can also explain the finite β stabilization of the electrostatic ITG. In fact, for increasing α (β), the coupling to the electromagnetic shear Alfvén branch also increases while, at the same time, the stabilizing influence of line bending diminishes (since the ideal marginal stability is approached). As a consequence, the stabilizing influence on the electrostatic ITG branch is expected to be strongest somewhere between $\alpha = 0$ and $\alpha = \alpha_{crit}$, as appears to be the case from Fig. 7. It could be argued that this should also be the point around which the most unstable mode should become that with an electromagnetic shear Alfvén polarization, although the electrostatic ITG cannot be generally expected to be completely stabilized.

As a concluding remark, it is worth emphasizing that low frequency ($\omega \approx \omega_{*pi} \approx \omega_{ti}$) shear Alfvén instabilities may have significant implications for both energetic and thermal particle transport. In the former case, as EPMS of either the BAE or the KBM branch, they may be candidates to explain the experimental observation [17] of large energetic ion losses due to Alfvén waves with frequencies lower than that of TAEs. In the latter case, the AITGs described in this section can be expected to particularly affect electron transport, since these modes are characterized by magnetic fluctuations and, in

contrast to electrostatic ITGs, are not stabilized by finite β effects.

References

- [1] Kieras, C.E., Tataronis, J.A., *J. Plasma Phys.* **28** (1982) 395.
- [2] Cheng, C.Z., Chen, L., Chance, M.S., *Ann. Phys.* **161** (1985) 21.
- [3] Mett, R.R., Mahajan, S.M., *Phys. Fluids B* **4** (1992) 2885.
- [4] Vlad, G., et al., *Nucl. Fusion* **35** (1995) 1651.
- [5] Connor, J.W., Hastie, R.J., Taylor, J.B., *Phys. Rev. Lett.* **40** (1978) 396.
- [6] Briguglio, S., et al., in *Fusion Energy 1996* (Proc. 16th Int. Conf. Montreal, 1996), Vol. 2, IAEA, Vienna (1997) 543.
- [7] Chen, L., in *Theory of Fusion Plasmas* (Vaclavik, J., Troyon, F., Sindoni, E., Eds), Editrice Compositori, Bologna (1989) 327.
- [8] Fu, G.Y., Cheng, C.Z., *Phys. Fluids B* **2** (1990) 985.
- [9] Zonca, F., Chen, L., *Phys. Fluids B* **5** (1993) 3668.
- [10] Chen, L., *Phys. Plasmas* **1** (1994) 1519.
- [11] Cheng, C.Z., Gorelenkov, N.N., Hsu, C.T., *Nucl. Fusion* **35** (1995) 1639.
- [12] Briguglio, S., et al., *Phys. Plasmas* **2** (1995) 3711.
- [13] Zonca, F., Chen, L., *Phys. Plasmas* **3** (1996) 323.
- [14] Briguglio, S., et al., *Phys. Plasmas* **5** (1998) 3287.
- [15] Santoro, R.A., Chen, L., *Phys. Plasmas* **3** (1996) 2349.
- [16] Turnbull, A.D., et al., *Phys. Fluids B* **5** (1993) 2546.
- [17] Heidbrink, W.W., Strait, E.J., Chu, M.S., Turnbull, A.D., *Phys. Rev. Lett.* **71** (1993) 855.
- [18] Biglari, H., Chen, L., *Phys. Rev. Lett.* **67** (1991) 3681.
- [19] Zonca, F., Chen, L., Santoro, R.A., *Plasma Phys. Control. Fusion* **38** (1996) 2011.
- [20] Tsai, S.T., Chen, L., *Phys. Fluids B* **5** (1993) 3284.
- [21] Mikhailovskij, A.B., *Nucl. Fusion* **13** (1973) 259.
- [22] Kotschenreuther, M., *Phys. Fluids* **29** (1986) 2898.
- [23] Zonca, F., Chen, L., Dong, J.Q., Santoro, R.A., in *Proc. Int. Sherwood Fusion Theory Conf. Atlanta* (1998) Paper 3B01.

(Manuscript received 12 November 1998

Final manuscript accepted 11 March 1999)

E-mail address of F. Zonca: zonca@frascati.enea.it

Subject classification: C0, Tt; D3, Tt; F2, Tt; F3, Tt